



Energy and temperature analysis in grinding

W.B. Rowe¹, M.N. Morgan¹, A. Batako¹ & T. Jin²

¹ *School of Engineering, Liverpool John Moores University, UK*

² *S.I.M.S. Cranfield University, UK*

Abstract

Energy consumption and dissipation are discussed, leading into a thermal model for grinding. The analysis developed over many years applies to shallow-cut conventional grinding processes and also to deep grinding processes. Energy analysis provides insights into the grinding process and suggests avenues for process improvements. The thermal model provides a good estimation of contact temperatures as well as temperatures on the finish surface. Case studies are presented to demonstrate how operational efficiency, component quality and removal rates are affected by process conditions.

Examples are included for High Efficiency Deep Grinding (HEDG). HEDG is defined as deep grinding at high workspeeds and very high removal rates. Tawakoli [20], Klocke [21]. The contact between the workpiece and wheel is represented as a circular arc. Experiments show that high removal rates and absence of thermal damage can be achieved. HEDG can achieve low specific grinding energy compared with shallow grinding and creep grinding. The chips take away most of the heat generated in the grinding process. As in creep grinding, burn-out of the coolant causes a steep rise in contact temperature of the workpiece.

1 Introduction

Cost, quality and productivity in grinding processes are all dependent on energy consumption and process efficiency. In an inefficient process, excessive heat leads to increased temperature rise in the workpiece causing problems with surface integrity and require more frequent interruptions of production. Excessive

energy consumption increases energy costs and demands an appropriate power transmission to the machine and heat extraction from the machine shop environment. On the other hand, many machines are underpowered. This has the consequence that removal rates must be reduced and the potential for high productivity is limited. This paper reviews the ways in which energy is dissipated in grinding processes. Dramatic differences between particular cases, demonstrate how quality and productivity are greatly affected, by the workpiece material, the machine speeds, the grinding wheel and the grinding fluid. Case studies are illustrated with temperature analysis.

Well-designed grinding processes usually enhance workpiece surface quality producing low roughness, compressive or neutral residual stresses and improved fatigue life. Grinding is a very efficient process for machining hard materials and has the potential to achieve high accuracy of shape and size.

Conversely, abusive machining can lead to a range of forms of surface damage. Generally, it is found that the higher is the machining temperature, the greater is the damage caused to the workpiece. Deleterious effects of high temperatures may include tensile residual stresses, increased roughness, oxidation, discoloration, softening or re-hardening of surfaces including brittle white layers and cracks. Other process-related problems are increased wheel wear, vibrations, loss of accuracy, reduced wheel life and reduced material removal rate. McCormack [1]

2 Energy input to the process

Power is one of the easier measurements on a modern machine tool. For convenience, the power is often represented as energy per unit volume of removed material often known as the specific energy or sometimes just as the energy.

Specific energy is a measure of process efficiency. It relates to the difficulty of machining a workpiece material. It also relates to wheel wear. For example, where the grinding power is 25 watts per cubic millimetre of material removed per second for a particular workpiece material, the specific energy is 25 J/mm^3 . For a harder-to-grind workpiece material being machined with a fine-grain wheel, the specific energy might be as high as 200 J/mm^3 . If the specific energy increases from 25 to 35 J/mm^3 , there has been a substantial deterioration in cutting efficiency, probably indicative of wheel glazing or wheel loading. This change is likely to be accompanied by deterioration in surface integrity. Alternatively, if the specific energy reduces from 25 to 20 J/mm^3 , there has been a substantial increase in cutting efficiency. This occurs when blunt edges of abrasive grains break away or whole grains are pulled out from the wheel and is accompanied by increased workpiece roughness. Either an increase or a reduction in specific energy is indicative of process problems, for example, with wheel wear or wheel dressing Webster [2], Chen [3]. A change will often be accompanied by other operational problems such as onset of vibrations, loss of

size control and defects such as surface softening, burn marks, re-hardening and cracking. Rowe [4].

The no-load power, P_{NL} is a combination of the windage, motor, transmission, bearing and fluid delivery losses. As the infeed commences, fluid comes into contact with the wheel and is accelerated towards wheel speed. This increases the power to the initial value at the start of grinding, P_{start} . As the feed continues, the removal rate increases until the total power reaches a maximum value, $P_{max.tot}$ as illustrated for a typical grinding cycle in Fig.1.

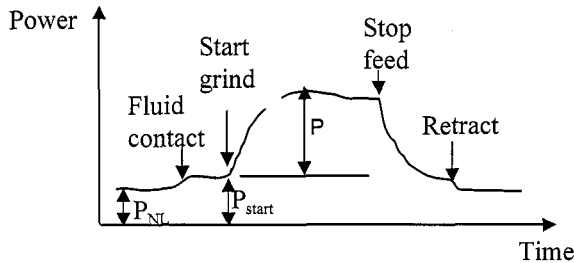


Figure 1: Maximum power in a typical infeed cycle.

The maximum grinding power,

$$P = P_{max.tot} - P_{start} \quad (1)$$

For a workspeed v_w , real depth of cut a_e and width of cut b_c , the material removal rate is,

$$Q_w = a_e \cdot b_c \cdot v_w \quad (2)$$

The specific energy is,

$$e_c = \frac{P}{Q_w} \quad (3)$$

A CNC can be programmed to monitor power, evaluate the specific energy and record values for subsequent inspection, provide warnings or take action. Rowe[5]

Specific energy input to the process depends on a number of factors principally related to the workpiece material and the cutting geometry of the grains. Some later examples will illustrate this point. To reduce specific energy, it is necessary to aim for,

- Large uncut chip thickness
- Sharp abrasive grains

6 Laser Metrology and Machine Performance VI

- A well lubricated process.

Adverse factors which increase specific energy are a lack of the above conditions and,

- High hot hardness of the workpiece material
- Chemical affinity between the workpiece and the grains leading to wheel loading
- Insufficient chip removal space in the surface of the abrasive tool
- A wheel with a hard bond, which retains grits when they are blunt.

Fig.2 shows a typical example of how specific energy is reduced with increasing depth of cut and removal rate in cylindrical grinding of cast steel. This tendency is found with most materials and may be interpreted in terms of the size of the chips removed by each cutting edge of the wheel. As the size of the chips increases, the energy required is reduced. This is known as the size effect. [6,7,8,9]

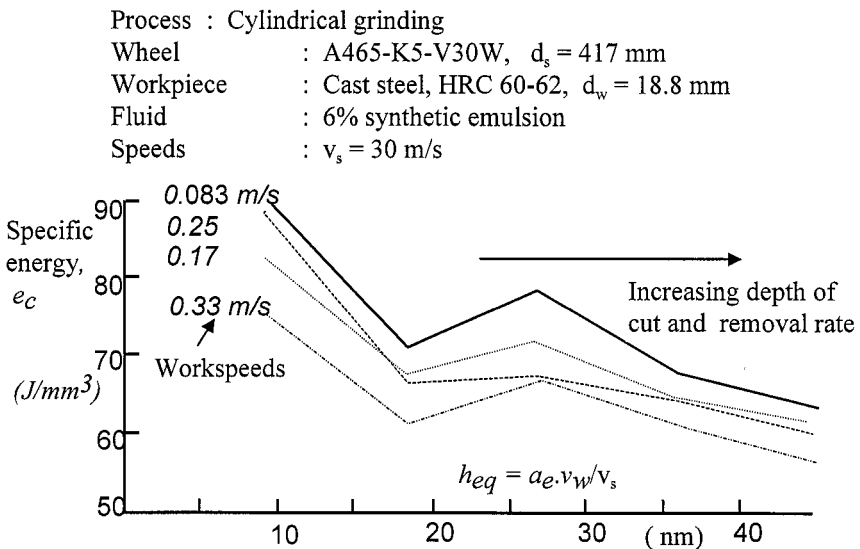


Figure 2: Effect of depth of cut and removal rate on specific energy.

There are several views on the size effect. Explanations are mainly based on,

- (i) The number of chips/unit volume removed - the sliced bread analogy: More slices take more energy. Rowe [8].
- (ii) Differences between cutting, ploughing and sliding: A refinement of the sliced bread analogy.
- (iii) A threshold force for cutting: Another variation.
- (iv) Grain sharpness: Efficiency increases with effective grain sharpness and hence with depth of grain penetration.

Hahn, [9] proposed three stages of material deformation as a grain interacts with a workpiece corresponding to sliding, ploughing and cutting. These are illustrated schematically in Figure 3.

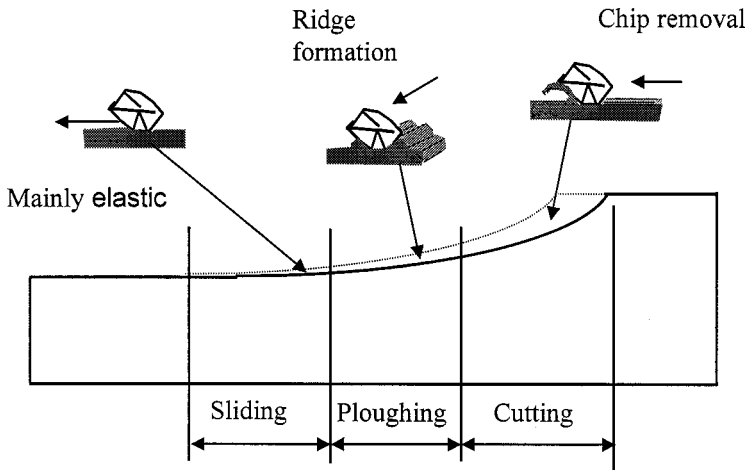


Figure 3: Sliding, ploughing and cutting regimes of grinding.

According to Malkin [10,11] the specific energy is the summation of sliding, ploughing and chip formation components from all the grain contacts taking place at any time,

$$e_c = e_{sl} + e_{pl} + e_{ch} \quad (4)$$

In the sliding mode of deformation, material removal is negligible although friction is apparent. Sliding or rubbing is typical of a polishing operation or finish grinding with a smooth wheel after a long period without application of a depth of cut with a well-lubricated surface. Elastic deformation and some plastic deformation take place at the peaks of asperities evidenced by polishing of the workpiece and a slow process of smoothing. Removal rate is very low and specific energy is very high.

Ploughing occurs when the penetration of the grains is increased. In the ploughing stage, scratch marks become evident and ridges are formed at the sides of the scratches. The scratch marks are evidence of significant penetration but the rate of material removal remains low and mainly due to fatigue. Removal rate is low and specific energy is high.

8 *Laser Metrology and Machine Performance VI*

As the penetration of the grains is further increased, material removal rapidly increases and chips are produced. The chip formation energy is much lower than the sliding and ploughing energy components. Hahn observed that there is a threshold force required before significant material removal takes place. With sharp grains the threshold force is low. With blunt grains the threshold force is high. The threshold force corresponds to the transition from sliding and ploughing to chip formation. As cutting depth is increased, the proportion of chip formation energy is increased compared with sliding and ploughing energy and the total specific energy drops.

The sliding, ploughing and cutting explanation can also be presented in terms of the cutting geometry of the grain. At small grain depth of cut, the grain presents a blunt geometry to the workpiece, which increases rubbing and ploughing relative to the cutting components of removal. As grain depth increases, the grain presents a sharper geometry to the workpiece and specific energy is reduced.

Process : Horizontal creep-feed grinding
Wheel : WA60/80FP2V,
Workpiece : C1023 nickel based alloy
Depth of cut : 4 mm
Speeds : $v_s = 30$ m/s, $v_w = 0.38$ microns per second

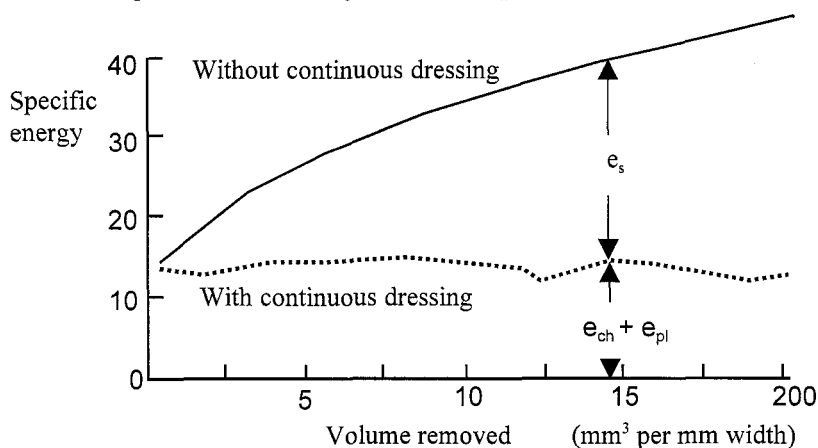


Figure 4: Specific energy with and without continuous dressing in creep-feed grinding. Based on Andrew, Howes and Pearce, 1985. [12]

The effect of wheel sharpness is highlighted by a creep-feed example from Andrew, Howes and Pearce [12]. C1023 Nickel-based alloy is a temperature resistant alloy used in the aerospace industry for turbine blades. Because the material is temperature resistant, it retains its hardness at higher temperatures. This increases specific energy required and wheel wear is rapid as shown in Fig 4. With continuous dressing, the wheel is constantly re-sharpened and the specific

energy remains low. Without continuous dressing, the wheel becomes blunt and the specific energy rapidly increases.

As the grains become dull, the specific energy is seen to increase rapidly from 150 J/mm³ to more than 400 J/mm³, powerfully demonstrating, the importance of grain sharpness.

3 Energy dissipation as heat

Power input to the process is dissipated as heat at the grain-workpiece interface. Heat spreads in the grinding contact area. The heat is conducted or convected by the workpiece, the wheel, the chips and the fluid.

The initial heat generation is virtually adiabatic leading to high grain contact temperatures approaching the workpiece melting temperature. Rowe [4]. This means the temperature of the grinding chips as they are produced is very much higher than the surrounding background temperature in the contact zone. It should be appreciated that the grain contact area for a sharp wheel is usually of the order of 1 to 3% of the contact zone area. Grain contact with a point on the workpiece lasts for the order of 1 microsecond. The very high grain contact temperature quickly decays to a local workpiece background temperature in the grinding contact zone. The background temperature is the result of many grain interactions. Contact between the wheel and an area of the workpiece is sustained typically over 100 microseconds. The related workpiece background temperature is therefore sustained over a relatively long period and can cause significant material damage to the workpiece surface.

The total heat flux distributed over the grinding contact area is shared between the workpiece, wheel, fluid and chips,

$$q_t = \frac{P}{A_c} = \frac{P_w + P_s + P_f + P_{ch}}{b_c \cdot l_c} \quad (5)$$

where the grinding contact area is given by $A_c = b_c \cdot l_c$ the product of the width and length of the grinding contact zone.

In order to identify the proportions of energy dissipated as heat through these four pathways, it is necessary to analyse the basic heat transfer mechanisms. This leads on to the estimation of workpiece temperatures.

4 Prediction of workpiece temperatures

4.1 Convection factors

The heat transfer to the workpiece, wheel fluid and chips is related to the maximum temperature of the workpiece and the mean chip temperature by convection factors, each to be evaluated,

10 *Laser Metrology and Machine Performance VI*

$$q_t = q_w + q_s + q_f + q_{ch} = h_w \cdot T_{\max} + h_s \cdot T_{\max} + h_f \cdot T_{\max} + h_{ch} \cdot T_{ch} \quad (6)$$

Mean temperatures can be estimated from T_{\max} rather than T_{mean} , assuming, $T_{\text{mean}} = 0.67T_{\max}$.

(i) The Workpiece. The heat flux into the workpiece can be expressed in the form, Carslaw [13]

$$q_w = \frac{\beta_w}{C} \cdot \sqrt{\frac{v_w}{l_c}} \cdot T_{\max} \quad \text{so that} \quad h_w = \frac{\beta_w}{C} \cdot \sqrt{\frac{v_w}{l_c}} \quad (7)$$

where, $\beta_w = \sqrt{k \cdot \rho \cdot c}$ is the thermal property of the workpiece material and C is a constant, which depends on Peclet Number and contact angle. See Appendix 1.

(ii) The Wheel. The heat flux to the wheel q_s can be related to q_w using Hahn's partition model for a grain sliding on a workpiece, [9,14]

$$q_s = q_w \cdot \frac{k_g}{\beta_w \sqrt{r_0 \cdot v_s}} \quad (8)$$

where, k_g is the thermal conductivity of the grains and v_s is the wheel speed. r_0 is the effective radius of the wear flats on the grains.

(iii) The Fluid. The convection factor for the fluid h_f depends on the type of fluid. In deep grinding 290,000 W/m²K gave good agreement between theory and experiment for water-based fluids and 23,000 W/m²K for oil [15,16]. However, if the mean workpiece temperature exceeds the boiling temperature of the fluid, it is found that complete burn-out occurs. The greatly reduced convection factor can then be assumed to be negligible. This transition occurs when the maximum temperature for wet grinding exceeds approximately 150% of the estimated fluid boiling temperature. For a water-based fluid, the transition occurs at a maximum temperature of about 180-200°C.

(iv) The Chips. The heat flux to the chips averaged over the contact area is proportional to the volume of chips removed and the chip temperature T_{ch} . The chip temperature is assumed to be 1500°C for ferrous materials [15] although

Stephenson [16], used values of 1000-1500°C. An average value of 1250°C might be assumed without serious loss of accuracy for most cases. Taking the mean value of specific heat from ambient to 1500°C, the chip energy for AISI1095 steel is estimated as 8.1 J/mm³. The value 6.75 J/mm³ for 1250°C gave better agreement in some cases.

$$q_{ch} = (\rho \cdot c \cdot a_e \cdot v_w / l_c) \cdot T_{ch} = e_{ch} \cdot a_e \cdot v_w / l_c \quad (9)$$

4.2 Maximum temperature equation

From eqns 6 to 9, the maximum temperature is established as,

$$T_{\max} = \frac{q_t - h_{ch} \cdot T_{ch}}{\frac{h_w}{R_{ws}} + h_f} \quad (10)$$

where, R_{ws} is the partition ratio of the workpiece-wheel sub-system.

4.3 Workpiece-wheel partitioning

The partitioning between the wheel and workpiece sub-system from Eqn 8 is,

$$R_{ws} = \frac{q_w}{q_w + q_s} = \frac{h_w}{h_w + h_s} = \left[1 + \frac{k_g}{\beta_w \sqrt{r_o \cdot v_s}} \right]^{-1} \quad (11)$$

where r_o represents an effective radius of contact of the abrasive grains. A value of 10 microns gives sensible results for a reasonably sharp wheel. The value of R_{ws} is not highly sensitive to the value of r_o unless much smaller values are selected.

For an alumina wheel grinding steel, R_{ws} is typically of the order of 0.9. For a CBN wheel, the value is reduced to approximately 0.5.

The ratio R_{ws} varies relatively slowly with r_o , whereas the fraction of heat R_w entering the workpiece, taking account of heat flows to the chips and fluid, is highly variable as will be evidenced in the case studies given below.

5 Heat conduction into the workpiece

5.1 Basic theory

For conventional grinding processes, the workpiece conduction factor can be calculated very easily from Eqn 7, since for high workspeeds and shallow cuts the value of C is approximately equal to 1.

12 *Laser Metrology and Machine Performance VI*

For deep grinding processes more accurate values are required. Accurate values for the conduction into the curved workpiece contact can be obtained by integrating the general equation for line heat sources moving at inclined contact angles ϕ_i , Fig 5.

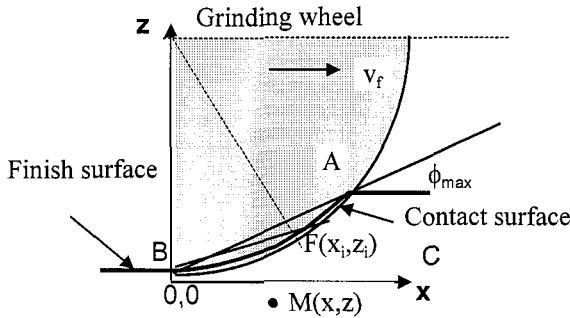


Figure 5: The curved heat source for grinding modelled as an infinite number of line sources along AB located at positions $F(x_i, z_i)$ and moving at an angle ϕ_i to the contact surface.

The contact surface is assumed to lie around a circular arc. The heat source is the summation of infinite moving line sources disposed around the contact arc. The contact length l_c , is arc AFB . A line source at $F(x_i, z_i)$ moves at speed v_w parallel to the x-axis at angle ϕ_i to the finish surface BC . The varying angle ϕ_i is the angle FBC , the maximum value of it along the arc AFB is the contact angle ϕ . The arc length, BF is $l_i = d_e \cdot \phi_i$ where d_e is the effective wheel diameter. The temperature rise at any point $M(x, z)$, due to the whole heat source AB , is

$$T = \frac{1}{\pi \cdot k} \int_0^{l_c} q \cdot e^{-\frac{v_w}{2 \cdot \alpha} (x - l_i \cos \phi_i)} K_0 \left[\frac{v_w \cdot r_i}{2 \cdot \alpha} \right] dl_i \quad (12)$$

$$\text{where } r_i = \sqrt{(x - l_i \cos \phi_i)^2 + (z - l_i \sin \phi_i)^2} .$$

K_0 is the Bessel function of second kind, order zero. α is thermal diffusivity and k is thermal conductivity.

The heat flux q is greatest at A and least at B. It is assumed to have the form

$$q = \bar{q} \cdot (n + 1) \cdot (l_i / l_c)^n \quad (13)$$

where $n = 0$ for a uniform heat flux and $n = 1$ for a triangular heat flux as applicable for grinding. \bar{q}_w is the mean heat flux entering the workpiece on the surface AFB.

For a rigid wheel and workpiece the contact length for deep cuts is given by, $l_c \approx \sqrt{a_e \cdot d_e}$. The contact angle may be estimated from the contact length and the effective wheel diameter:

$$\phi = l_c / d_e \quad (14)$$

The effective wheel diameter is given by $\frac{1}{d_e} = \frac{1}{d_s} \pm \frac{1}{d_w}$. A positive sign applies for external grinding and a negative sign applies for internal grinding.

Equation 12 can be expressed in dimensionless form with

$X = \frac{v_w \cdot x}{4 \cdot \alpha}$, $Z = \frac{v_w \cdot z}{4 \cdot \alpha}$, and Peclet Number $L = \frac{v_w \cdot l_c}{4 \cdot \alpha}$ so that, dimensionless temperature is

$$\bar{T} = \frac{\pi \cdot k \cdot v_w}{2 \cdot \alpha \cdot \bar{q}_w} \cdot T \quad (15)$$

5.2 Dimensionless workpiece temperature values

Using a maths package, Eqn 12 provides temperatures along the contact surface AFB and along the finish plane BC. Other temperatures can be obtained as required. Values are given in Fig 6 for a range of contact angles and Peclet Number $L=50$.

These dimensionless values give actual temperatures depending on the heat flux entering the workpiece.

$$T = \frac{2 \cdot \alpha \cdot P_w}{\pi \cdot k \cdot v_w \cdot b_c \cdot l_c} \cdot \bar{T} \quad (16)$$

Increasing contact angle for a particular power per unit area reduces contact temperature and temperature on the finish surface. The contact angle is larger in external cylindrical grinding than in internal grinding which indicates a more favourable condition.

High workpiece speeds reduce temperatures while high removal rates increase power and tend to increase temperatures. High contact angles and high workpiece speeds tend to imply high removal rates so that temperatures tend to go up.

14 *Laser Metrology and Machine Performance VI*

However, specific energy tends to be reduced as removal rate increases so under particular conditions, there is the possibility to reduce temperatures as shown below.

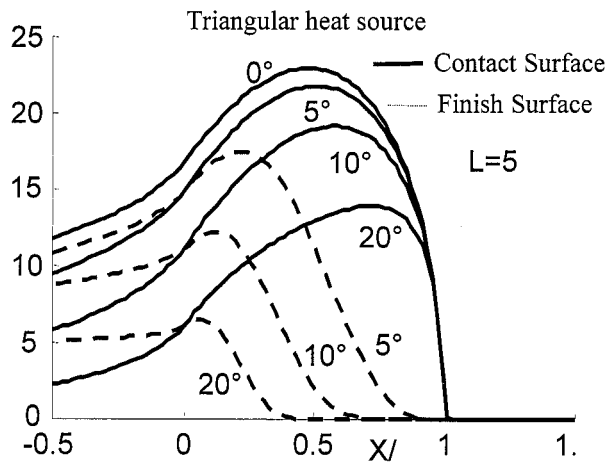


Figure 6: Dimensionless temperatures for workpiece conduction on the contact and finish surfaces.

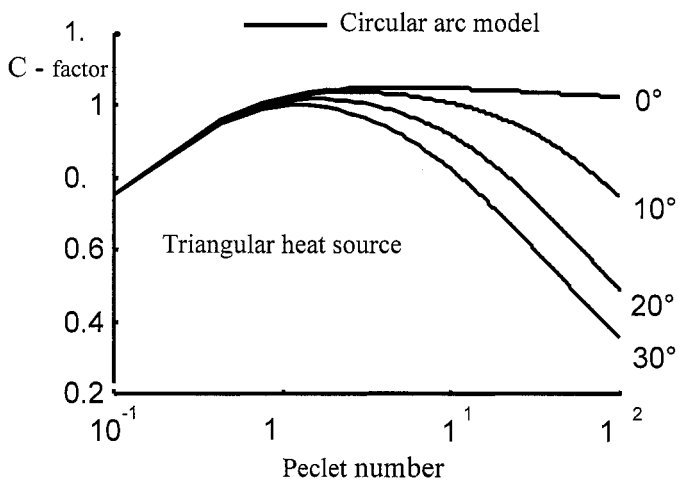


Figure 7: C-Factors for maximum temperature on contact surface, Eqn 7.

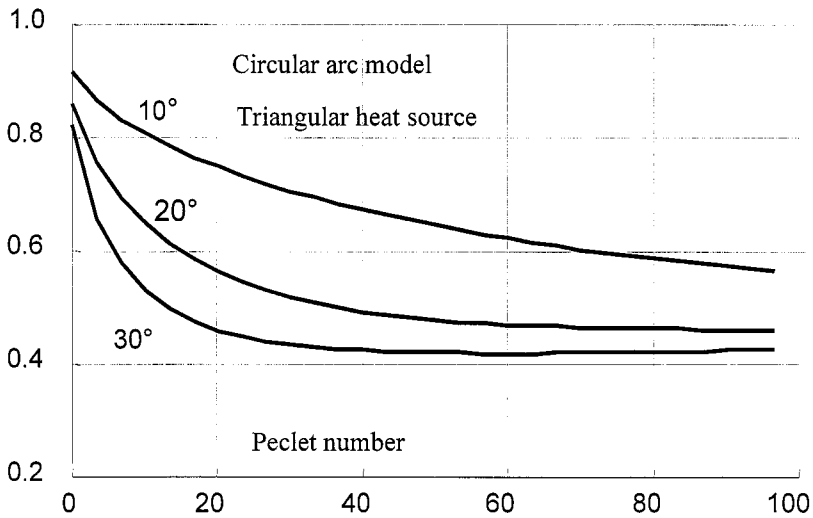
$T_{fin.max}/T_{cont.max}$ 

Figure 8: Maximum temperatures on the finish surface, $T_{fin.max}$ as a fraction of the maximum contact temperature, $T_{cont.max}$.

Although Fig 5, gives workpiece conduction values for $L=50$, further values are required to cover the full range of grinding conditions including creep-grinding, HEDG and conventional grinding.

A large number of results are condensed in Figs 6 and 7. Using the values in these figures and the thermal properties of the workpiece, wheel and fluid, it is possible to estimate grinding temperatures for a wide range of process conditions.

6 Comparison between theory and experiment

As the technology of temperature measurement has advanced, considerable progress has been made in refining and calibrating the thermal model. In order to make predictions, it is required to know the specific energy of the process and the fluid heat convection factor. So far, it has been impossible to calculate these values from a purely theoretical approach. However, process power can be monitored allowing specific energy to be evaluated as grinding proceeds and convection factors have been estimated by comparing temperature predictions with experimental values for a range of grinding results. Using this approach it is then possible to use the thermal model to estimate maximum temperatures.

Fig. 9, illustrates an example for shallow cut grinding using a water-based fluid. It is seen that the thermal model gives good agreement between theory and experiment for a range of depths of cut. In this example no allowance was made



16 *Laser Metrology and Machine Performance VI*

for fluid convection. It therefore appears that the fluid delivery was relatively ineffective and that burn-out had taken place for all depths of cut.

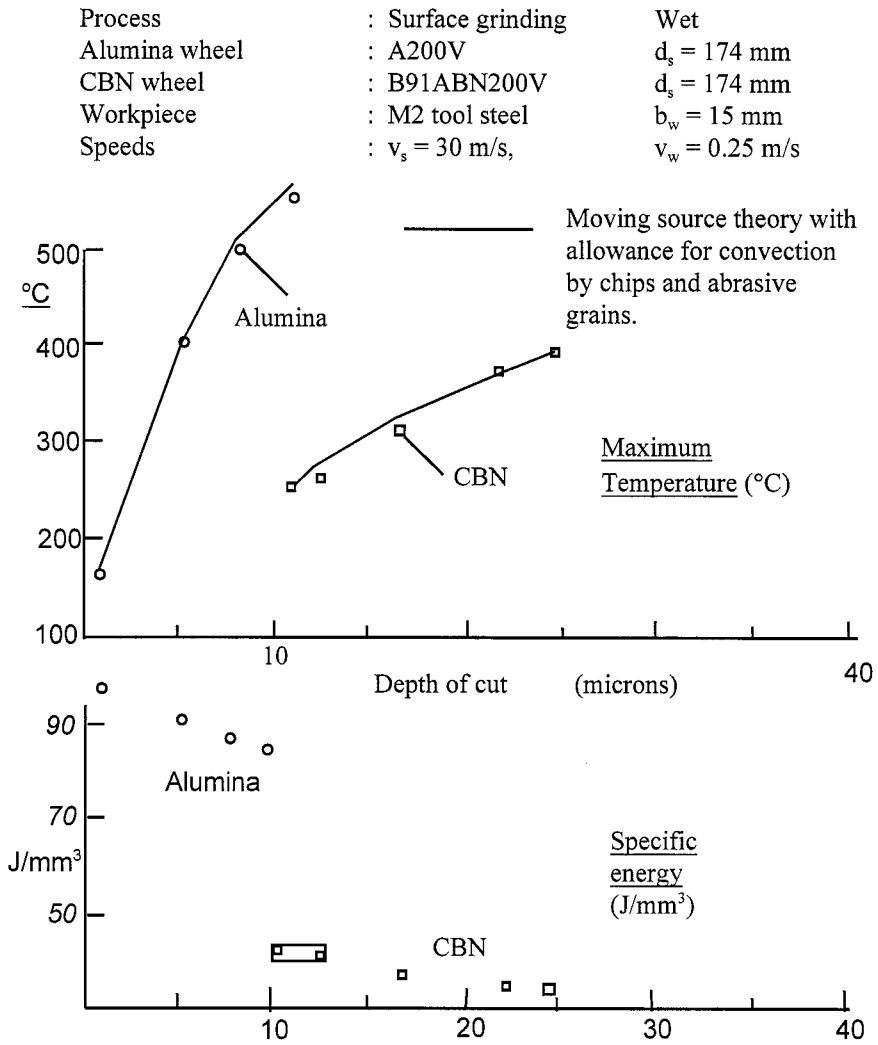


Figure 9: Effect of depth of cut on temperature, T_{max} , for a case where the specific energy with CBN is lower than with an alumina wheel.

Table 1: Approximate thermal properties of typical abrasive grains.

	Conductivity (W/mK)	Density (kg/m ³)	Spec. heat (J/kgK)	$\beta = \sqrt{k \cdot \rho \cdot c}$ (J/m ² sK)
Diamond	2000	3520	511	60000
CBN	240	3480	506	20600
Pure CBN - up to 1300				48000
Silicon carbide	100	3210	710	15100
Aluminium oxide	35	3980	765	10300

Table 2: Thermal properties of typical engineering materials at room temperature.

	Conductivity: (W/mK)	Density: (kg/m ³)	Spec heat: (J/kgK)	$\sqrt{k \cdot \rho \cdot c}$ (J/m ² sK)	α ($\times 10^{-6}$)
Cast iron (260)	53.7	7300	511	14150	14.4
AISI 1055	42.6	7840	477	12600	11.4
AISI 1095	41	7870	560	13440	9.3
M2 tool steel	23.5	7860	515	9750	5.80
AISI 52100	34.3	7815	506	11650	8.67

Four case studies of estimated temperatures and experimental temperatures are given in Table 3. Approximate thermal properties of typical abrasive grains and of workpiece materials are listed in Tables 1 and 2. Thermal conductivity and specific heat values vary with temperature, while the thermal property, $\beta = \sqrt{k \cdot \rho \cdot c}$, varies much less. The non-steady-state property, β_w is appropriate for heat transfer to the workpiece. Constant mean values were assumed.

Abrasive grains quickly reach quasi-steady state, so steady-state thermal conductivity must be used rather than the non-steady-state parameter, β_s . A value was used for temperature close to workpiece melting which is the approximate temperature at the grain contact.

All four case studies illustrate removal processes where the integrity of the workpiece surface is maintained. No thermal damage occurred in any of these examples. However, the removal rates are greatly different.

Table 3: Comparison of estimated and measured temperatures in grinding.

Process/Parameter	Shallow	Creep	Creep	HEDG
Source of data	Black[17]	Kim[18]	Ohishi[19]	Rowe
depth of cut : mm	0.012	0.5	1	0.96
wheel dia : mm	200	350	305	170
workspeed, : m/s	0.3	0.005	0.0006	0.3
contact length : mm	3.10	13.2	17.5	12.8
contact time : s	0.01	2.65	29.1	0.043
L=Peclet number	27	1.6	0.15	103
remov. rate/width: mm ² /s	3.6	2.5	0.6	288
spec. energy :J/mm ³	60	67	190	11.0
power/width :W/mm	216	168	114	3168
q _r =power/area :W/mm ²	69.7	12.7	6.53	248
PHI :degrees	0.22	2.17	3.28	4.31
C-factor for workpiece HT	1.1	1.04	0.81	0.75
abrasive type	cBN	alumina	alumina	alumina
Rws: Subsystem partition	0.46	0.88	0.85	0.89
hw :W/m ² K	104214	8325	3277	75274
process fluid	emulsion	emulsion	oil	emulsion
hf :W/m ² K	10000	290000	23000	290000
q _{ch} =h _{ch} .T _{mp} :W/mm ²	6.9	1.1	0.18	184
Tmax - dry : °C	275	1222	1641	763
Tmax - wet : °C	264	38	236	172
Tmax - measured : °C	320	40	260	180
Tfin.max/Tcont.max	1	0.95	0.98	0.82
Tfin.max : °C	275	37	232	141

(i) **Shallow-cut grinding.** The first column shows shallow-cut grinding at a removal rate of 3.6 mm³/s per mm wheel width using a CBN grinding wheel [Black, 17]. CBN is a very good heat conductor and the partition ratio R_{ws} of the wheel-workpiece subsystem has the low value of 0.46. The predicted temperature rise of 275°C ignoring fluid convection gives reasonable agreement with the

measured value of 320°C. The fluid convection is ignored because the estimated temperature is approximately double the boiling temperature of a water-based fluid. In this example, it appears that the chips do not remove more than 10% of the total heat flux. The two main routes for heat dissipation are the wheel and the workpiece.

Assuming a relatively low fluid convection coefficient of 10,000 W/m²K for shallow-cut grinding, fluid convection makes little difference to the temperature estimate. Using the value of 290,000 W/m²K for fluid convection reduces the predicted temperature rise to 120°C. This temperature would not be high enough to cause complete burn-out for a water-based emulsion in a deep grinding process. It appears that fluid convection in shallow-cut grinding may not always be as effective as it is in deep grinding processes. Most shallow-cut grinding processes take place at temperatures above boiling and therefore convection has not been given the attention it deserves. Further work is required for low temperature shallow-cut grinding to clarify this point. Other grinding results from this series of tests showed that emulsion was effective in reducing the specific energy compared with dry grinding but was not effective in providing a high value convection coefficient, presumably due to burn-out.

(ii) Creep-grinding. Two examples of creep grinding using alumina wheels are given. Creep grinding with oil at a 1 mm depth of cut removed material at a modest rate of 0.6 mm³/mm.s at the very slow workspeed of 0.0006 m/s. The maximum temperature measured was 260°C in spite of the very high specific energy of 190 J/mm³.

Creep grinding with a water-based emulsion at a workspeed of 0.005 m/s achieved a lower specific energy of 67 J/mm³ and a rather higher removal rate of 2.5 mm³/mm.s. As a consequence of the low specific energy and the high convection cooling, the maximum temperature measured was 40°C.

Alumina wheels give a high wheel-workpiece partition ratio of 0.85 compared to a value of 0.46 for CBN. The removal rates in these creep grinding examples are similar to values commonly employed in shallow-cut grinding. As in shallow-cut grinding, the chip energy is a small proportion of the total energy. However, in the two examples, it can be seen that fluid convection plays a very important role. The predicted temperature for dry grinding in Kim's result, [18] is 1222°C compared with 38°C for wet grinding with a water-based fluid. Ohishi's result [19] for creep grinding with neat oil shows a similar importance of fluid convection. In creep grinding, fluid convection is very important in keeping temperatures down to an acceptable level. However, it is clear that low temperature grinding can be achieved even at 1 mm depth of cut.

(iii) HEDG. High-efficiency deep grinding is conducted at high workspeeds compared to creep grinding. The combination of deep cuts and high workspeeds implies extremely high removal rates. In the example shown, the removal rate of 288 mm²/s is approximately 100 times larger than the previous examples.

To cope with the high removal rates wheelspeeds are normally increased to the highest values practicable to reduce the problem of rapid wheel wear. The above case study was undertaken with the relatively low wheelspeed of 55 m/s. The cost, was rapid wear of the grinding wheel making it more difficult to maintain workpiece accuracy. Wheelspeeds up to 200 m/s have been employed for deep grinding using special high-speed alumina and CBN wheels.

A particular feature experienced in HEDG is that specific energy is reduced. The specific energy in this example was 11 J/mm³ compared with 60 to 190 J/mm³ in the previous cases. A full explanation of the reduced specific energies in HEDG remains to be determined. Self-sharpening with high wheel wear rates characterise the process using conventional wheels and help to explain the low specific energies. Electroplated CBN wheels do not suffer such high wear rates and yet low values of specific energy are still experienced. There must therefore be an additional explanation. It may be that low specific energy is at least partly a thermal phenomenon related to material softening in a very thin layer along the arc of contact.

Thermal analysis shows that HEDG relies for its success on achievement of a very low specific energy. Very low specific energy means that the total process energy is of the same order of magnitude as the chip energy. This means that the heat carried away by the chips reaching a temperature close to melting is a large proportion of the total heat. In the above case study, it is estimated that the chips carry away approximately 75% of the total heat flux. 21% is convected mainly by the fluid leaving approximately 4% to the wheel and workpiece.

The high value of fluid convection coefficient gives good agreement with experiment. The model also shows that the maximum temperature on the finish plane is approximately 30°C lower than the temperature on the contact surface.

Some further examples of temperature measurement for HEDG are shown below. The test conditions are listed in Table 4. The test set-up is illustrated schematically in Fig 10. Experiments were conducted on a 6 kW surface grinder using an alumina wheel. Workpieces were made of two steel strips, sandwiching a constantan wire of 25 µm diameter to form a J-type thermocouple. Workpieces were 1.2 mm wide giving a narrow aspect ratio. However, two-dimensional heat transfer basically applies with this section.

Table 4: Test conditions

Wheel	: 73A601 18V LNAA, 169~174 mm dia.
Wheel speed	: 55 m/s
Worktable speed	: 0.2~0.32 m/s
Depth of cut	: 0.4~1 mm,
Dresser	: Single point diamond
Dressing depth	: 0.015 mm
Dressing feed	: 12 mm/s
Coolant	: Hysol X-10% Emulsion
Workpiece	: AISI 1095

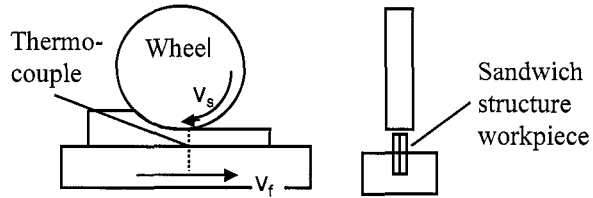


Figure 10: Experimental set-up.

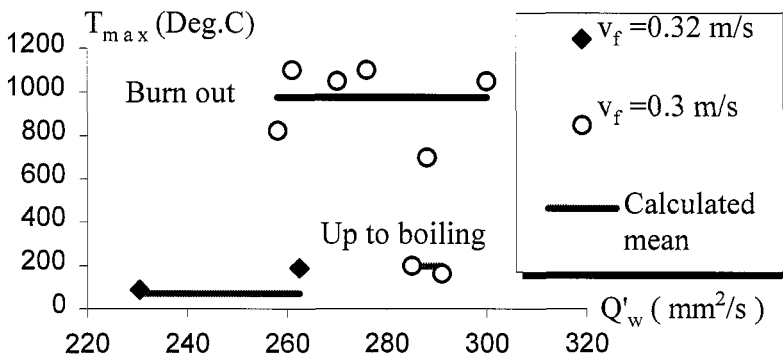


Figure 11: Measured maximum contact temperatures in near-transitional conditions.

The experiments were conducted for conditions close to fluid burn-out. It can be seen there is a jump from low-temperature grinding to high-temperature grinding. This is exactly, as predicted by the thermal model. It is interesting that with effective fluid delivery, it is possible to keep temperatures very low, even at extremely high removal rates.

7 Conclusions

The crucial importance of energy in a grinding process has been highlighted. The abrasive, wheel design, dressing strategies and grinding conditions can all strongly affect energy.

Energy and temperature analysis reveals remarkable differences between grinding processes. In conventional grinding, most of the heat goes into the workpiece. This means that thermal damage often results and coolant convection may be ineffective.



In high-efficiency deep grinding, this situation is changed. Under the right conditions, it is possible to reduce specific energy and achieve remarkably high material removal rates with low temperatures using high wheelspeeds and high workspeeds.

In industrial practice, much larger depths of cut are achieved with more powerful machines than are available in most laboratories. An advantage of a large depth of cut and a high workspeed is the lower temperature on the finish surface compared with the maximum temperature experienced on the contact surface. However, it is of critical importance that specific energy is reduced to a very low level and conditions for cool grinding are achieved.

Examples have been quoted for successful achievement of remarkable removal rates using high-efficiency deep grinding. However, it cannot be claimed that HEDG is a routine procedure. Further research is required to fully establish the principles governing HEDG.

Temperature analysis has led to new insights. Background maximum temperature under burn-out conditions approaches but is always less than melting temperature. Grain contact temperatures approach but cannot exceed melting temperature tending to limit specific energy. Specific energy at its lowest values, approaches the melting energy of the chips.

The circular arc heat conduction model improves temperature estimation compared to a sliding source or a straight inclined plane model. Reasonable agreement between theory and experiment for deep grinding can only be achieved when taking all factors into account, including fluid convection, chip energy convection, conduction into the abrasive and the circular arc contact model.

The transition from boiling to burn-out of the coolant has a strong influence on contact temperatures. Results indicate that fluid convection factors can be extremely high as boiling conditions are approached. After burn-out fluid convection is greatly reduced.

References

- [1] McCormack, D., Rowe, W. B., Jin, T. Controlling the Surface Integrity of Ground Components. *Society of Manufacturing Engineers Paper MR01-236, 4th Int Machining & Grinding Conference*, 2001,.
- [2] Webster, J., Brinksmeier, E., Heinzl, C., Wittman, M., Thoens, K., Assessment of Grinding Fluid Effectiveness in Continuous-Dress Creep Grinding, *Annals of the CIRP*, 51, 1, 235-240, 2002,.
- [3] X Chen, "Strategy for Selection of Grinding Wheel Dressing Conditions" *PhD thesis, Liverpool John Moores University*. 1995,
- [4] Rowe, W.B., Marinescu, I., Dimitrov, B., Inasaki, I., Grinding and Tribology of Abrasive Machining Processes, *William Andrew Publishing, Norwich, NY*, 2003,

- [5] Rowe, W.B., An Open CNC Interface for Grinding Machines, *Int. J. of Manufacturing Science and Technology*, 1, 1, 17-23, 1999,.
- [6] Chen, C., Jung, Y., Inasaki, I, Surface ,Cylindrical and Internal Grinding of Advanced Ceramics” *Grinding Fundamentals and Applications*, Trans ASME, 39, 201-211, 1989.
- [7] Backer, W.R., Marshall, E.R., Shaw, M.C., “The Size Effect in Metal-cutting”, *Trans ASME*, 74, 61-72. 1952
- [8] Rowe, W.B., Chen, X., “ Characterization of the Size Effect in Grinding and the Sliced Bread Analogy” *Int. J. Production Research*, 35, 3, 887-899, 1997.
- [9] Hahn, R S. “ On the Mechanics of the Grinding Process Under Plunge Cut Conditions” *Trans ASME, Journal of Engineering for Industry*, 72-80,1966.
- [10] Kannapan and Malkin, S., “Effects of grain size and operating parameters on the mechanics of grinding” *Trans ASME, Journal of Engineering for Industry*, 94, 833-842, 1972.
- [11]Malkin, S., “*Grinding Technology*” Ellis Horwood. 1989.
- [12]Andrew, C., Howes, T., Pearce, T., “*Creep feed grinding*”, Holt, Rinehart and Winston. 1985
- [13]Carslaw, H., Jaeger, J. C., Conduction of Heat in Solids, *Oxford Science Publications*, Oxford University Press. 1959.
- [14]Rowe, W. B., Morgan, M. N., Black, S. C. E., Mills, B., A Simplified Approach to Thermal Damage in Grinding, *Annals of the CIRP*, 45/1: 299-302. 1996.
- [15]Rowe, W. B., Jin, T., Temperatures in High-Efficiency Deep Grinding, *Annals of the CIRP*, 50,1, 205-208. 2001
- [16]Stephenson, D.J., Jin, T., Corbett, J., , High-Efficiency Deep Grinding of a Low-Alloy Steel with Plated CBN Wheels, *Annals of the CIRP*, 51, 1, 241-244. 2002.
- [17]Black, S.C., The Effect of Abrasive Properties on the Surface Integrity of Ground Ferrous Materials, *PhD thesis, Liverpool John Moores University*. 1996.
- [18]Kim, N.K., Malkin, S., Heat Flux and Partition in Creep-Feed Grinding, *Annals of the CIRP*, 46, 1, 227-232. 1997.
- [19]Ohishi, S., Furukawa, Y., Analysis of Workpiece Temperature and Grinding Burn in Creep-Feed Grinding, *Bulletin of JSME*, 28,242, 1775-1781. 1985.
- [20]Tawakoli, T., High Efficiency Deep Grinding, *VDI-Verlag and Mechanical Engineering Publications Limited (MEP)*. 1993.
- [21]Klocke, F., Brinksmeier, E., Evans, C., Howes, T., Inasaki, I., Minke, E., Tönshoff, H. K., Webster, J.A., Stuff, D., High-Speed grinding - Fundamentals and State-of-the-Art in Europe, Japan and the USA , *Annals of the CIRP*, 46/2:715 - 724 .1997.

